Presented at ICALEO'99.
San Diego, USA, November 15-18, 1999.
Session 6: Sensing & Monitoring II.

Multivariable control of laser alloying of Ti6Al4V

G.R.B.E. Römer, J. Meijer and R.G.K.M. Aarts
University of Twente, Department of Mechanical Engineering
P.O. Box 217, 7500 AE, Enschede, the Netherlands

Abstract

The results of laser surface alloying of titanium with nitrogen gas may vary significantly during processing due to variations in absorptivity and geometrical variations of the work piece. To increase the reproducibility of the process, a real-time feedback control system was designed and tested. Process models were developed to gain insight in the process behavior. As a test case, laser alloying of titanium (Ti6Al4V) with nitrogen was applied. The quantities, which have been measured, are the temperature and the melt pool surface area. For the process result, however, quantities as layer thickness and homogeneity are of more interest. Dynamic and steady state models have been developed to relate the processing results to the measured quantities. A thermographic CCD camera was applied to measure the melt pool surface area. One and two color pyrometers were used to measure the surface temperature. The effects of the laser power, the beam velocity and disturbances in absorptivity and work piece geometry were analyzed theoretically, as well as experimentally. Both the width and length of the pool area varies due to the disturbances. In the case of a thin work piece, the length varies more than the width. In the case of an absorptivity disturbance, the variation of the length and width are of the same order. As a result, it was found that the laser power is the appropriate actuator to control absorptivity disturbances. The beam velocity can be best applied to suppress the effects introduced by geometrical variations of the work piece. Based on these results, several controller algorithms were implemented and tested. It is shown that a multivariable mode-switch controller produces the most stable results.

1 Introduction

It is well known that the results of laser surface treatment may vary significantly even under apparently constant processing conditions. This due to the high sensitivity of laser surface treatment to process disturbances. As a result, the desired temperature cycle and temperature distribution of the work piece is perturbed, which may induce unacceptable process errors. The major process disturbances are varying absorptivity and a complex work piece geometry. The absorptivity of metals for CO_2 laser radiation (typically 10%) may vary considerably during processing.[1] This perturbs the temperature cycle significantly. When a work piece with small dimensions (e.g. a thin wall) is treated the self quenching capacity is reduced. This results in a perturbation of the temperature cycle. An approach is to consider the geometry as semi-infinite and the perturbations due to geometrically small dimensions as process disturbances. Reproducible results (e.g. constant surface layer thickness) can be achieved by feedback control. The most important quantity, however, the layer thickness can not be measured on-line. Quantities, which can be readily measured on-line, are temperatures and temperature profiles. Therefore, the processing results should be related to the induced temperature cycle of the surface layer. For processes including a liquid phase, the results not only depend on the temperature cycle, but also depends on the shape and dimensions of the melt pool.[2] When it is assumed that the beam velocity is constant, constant processing results can be obtained if the temperature distribution is maintained constant. Then the objective of the control system can be reformulated as to obtain a constant temperature distribution in the surface layer, despite disturbances. In the case of a laser generated melt pool, an additional requirement is to obtain constant melt pool dimensions. Input quantities, which can be commanded relatively easily with

todays CNC's are laser power and relative beam velocity. Then the laser source and the product manipulator are the corresponding actuators.

In this paper feedback control of the alloyed layer thickness in laser alloying of Ti6Al4V with nitrogen forming titanium-nitride (TiN) is considered.[3]

2 Process modelling

Process models are required to analyze the effects of the laser power P_L, the beam velocity v, as well as the disturbances (absorptivity A, small geometry) on the quantities as temperature, melt pool geometry, etc. Moreover, a dynamic process model is an absolute requirement for the design of a controller. The physics of laser surface treatment are described by the laws of conservation of energy (heat conduction equation), momentum (Navier-Stokes) and mass. In most cases, the influence of radiant heat losses and the effects of additional material on the temperature distribution can be neglected. Then, to obtain a first approximation of the temperature distribution T, the melt pool and its direct surroundings can be modelled as a volume, with increased heat conductivity K (to account for the effect of heat transport by convection in the melt pool[4]), and an increased specific heat c_p (to account for the heat of fusion and reaction energy in the case of a chemical reaction in the melt pool[5]). These simplifications result in the well known heat conduction equation. Unfortunately, the solution to of the 3D heat conduction equation can not be calculated in explicit form for an arbitrary laser beam intensity profile. Therefore the static ($\partial T/\partial t = 0$) and dynamic ($\partial T/\partial t \neq 0$) solutions are discussed separately in the following.

2.1 Steady state solution

The steady state ($\partial T/\partial t = 0$) solution of the heat conduction equation, when expressed in dimensionless coordinates in a coordinate system fixed to the laser beam, reads[5]

$$\theta(\chi,\eta,\zeta) = \frac{2}{d_x^{3/2}\sqrt{d_y}} \int_{-\infty}^{\infty}\int_{-\infty}^{\infty} \frac{\Phi(\chi',\eta')}{\psi} \exp\left[-\frac{\mathrm{Pe}}{4}(\chi-\chi'+\psi)\right] d\chi' d\eta', \tag{1}$$

with $\psi = \sqrt{(\chi-\chi')^2+(\eta-\eta')^2+\zeta^2}$, and where $\chi = 2x/d_x$, $\eta = 2y/d_x$, $\zeta = 2z/d_x$ denote the dimensionless equivalents of the coordinates (x,y,z), d_x and d_y denote the width and length of the intensity profile $I(x,y)$ respectively. The Peclet number $\mathrm{Pe} = (d_x v)/\kappa$ is applied as the dimensionless beam velocity with κ the thermal diffusitivity. The dimensionless intensity profile equals $\Phi(\chi,\eta) = d_x d_y I(\chi,\eta)/(4AP_L)$. The temperature distribution T in the work piece is related to its dimensionless equivalent as $\theta(\chi,\eta,\zeta) = K\pi\sqrt{d_x d_y}\,T(\chi,\eta,\zeta)/(2AP_L)$.

The dimensionless temperature distribution (1) does not depend on laser power P_L. This implies that only the amplitude of the temperature distribution depends on the laser power and not the distribution itself. The same is concluded for the dependency on the absorptivity A. This means that for the suppression of absorptivity disturbances, the laser power is the most appropriate input command.

Figure 1 shows three normalized surface temperature distributions induced by a laser beam with a top hat intensity profile. The temperature distribution in the plate was calculated by (1) using of image heat sources.[6] The the surface temperature distribution in the plate (dotted curve) resembles that of the fast moving beam in the infinite work piece (dashed curve). This means that for high velocities the plate may be considered as a semi-infinite work piece. We will take advantage of this effect by using the beam velocity v to suppress the negative effects caused by a geometrical disturbance (work piece of reduced thickness).

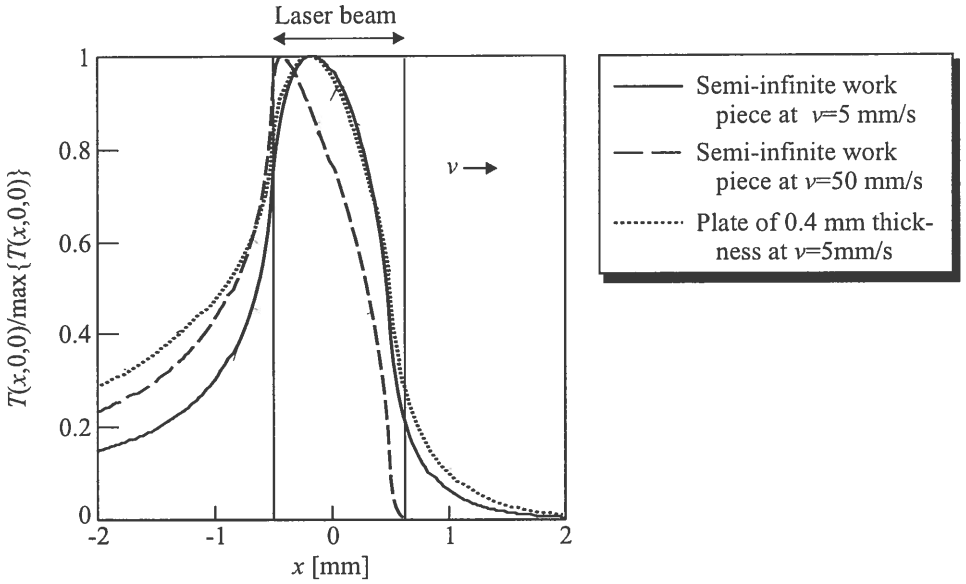

Figure 1: Normalized longitudinal surface temperature in Ti6Al4V, induced by a circular uniform intensity profile (top hat) with $AP_L = 35\,W$ and beam diameter $d = 1\,mm$, at two beam velocities and two work piece geometries.

2.2 Dynamic process model

The design of a feedback controller requires a dynamic process model. Two transfer functions, relating the input signals (laser power and beam velocity) to the temperature distribution can be distinguished

$$G_{P_L}(s) = \left.\frac{T(x,y,z,s)}{P_L(s)}\right|_{v=\text{const.}} \quad \text{and} \quad G_v(s) = \left.\frac{T(x,y,z,s)}{v(s)}\right|_{P_L=\text{const.}}, \tag{2}$$

where s is the Laplace or frequency variable and $T(x,y,z,s)$, $P_L(s)$ and $v(s)$ are the corresponding Laplace transforms with respect to time. Unfortunately, an explicit expression for $T(x,y,z,s)$ cannot be derived analytically for an arbitrary intensity profile. However, the temperature distribution, and the transfer function G_{P_L}, for a point source, $I(x,y,t) = P_L H(t)\delta(x)\delta(y)$, with H the Heaviside step function and δ the Dirac function, can be derived[7]

$$G_{P_L}(s) = \frac{1}{2\pi K\vartheta}\exp\left[-\frac{vx+\vartheta\sqrt{4s\kappa+v^2}}{2\kappa}\right], \vartheta = \sqrt{x^2+y^2+z^2}. \tag{3}$$

The transfer function corresponding to a laser beam with intensity profile $I(x,y)$ follows from the weighted sum of the transfer functions (3). It can be shown that for low frequencies transfer function (3) may be approximated by a first order rational transfer function.[7] This first order model will be determined through system identification (see section 4). Also, transfer function $G_v(s)$ (2) is hardly to derive analytically. Therefore, this transfer function was also determined through system identification.

3 Experimental setup

Figure 2 shows the experimental setup. A CO_2 laser source (TEM_{01^*}+TEM_{00}), with measured power rise time $t_r \approx 22\,\mu s$, was applied. The spot diameter on the surface was $d = 1.1\,mm$. The Ti6Al4V samples (⌀40 by 4 mm) were sandblasted and mounted on a XY-table. Nitrogen gas is supplied by

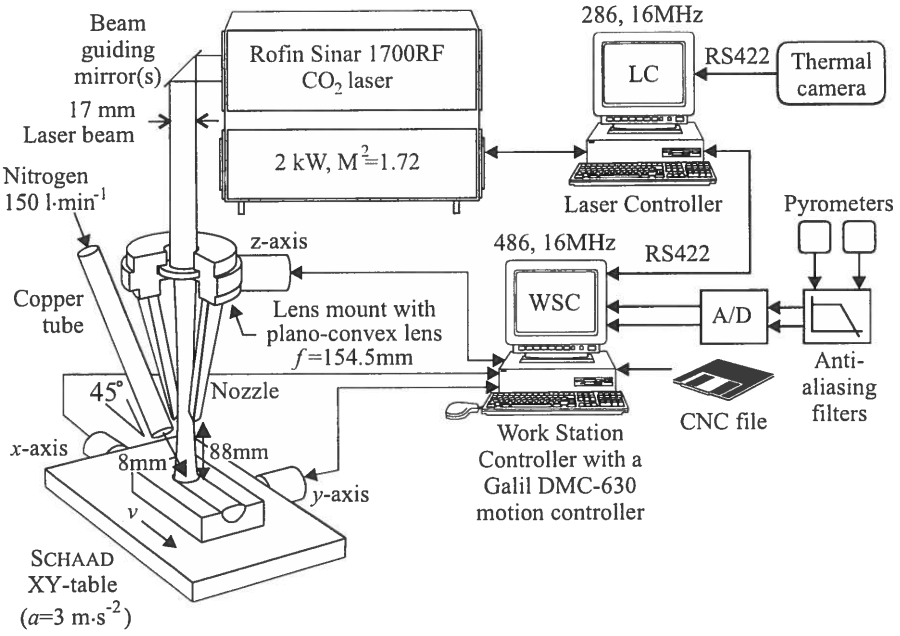

Figure 2: The experimental set-up.

a tube from aside. A thermographic CCD camera (128×128, $\lambda \approx 950\mu$m) was used to measure the melt pool surface area.[8] In addition, two pyrometers were applied to monitor the process: a spectral pyrometer ($\lambda = 0.975\,\mu$m, rise time $t_r \approx 0.3$ms) and a ratio pyrometer ($\lambda = 0.95\,\mu$m & $\lambda = 1.05\,\mu$m, spot size Ø0.45mm, rise time $t_r \approx 10$ms).

4 Process behaviour

Experiments showed that the melt pool surface area S_m is linearly correlated to the depth.[9] Figure 3(b) shows the isotherms of the laser-material interaction zone of a work piece which was covered with a graphite coating (3μm). Compared to an unperturbed work piece (fig. 3(a)), merely the area

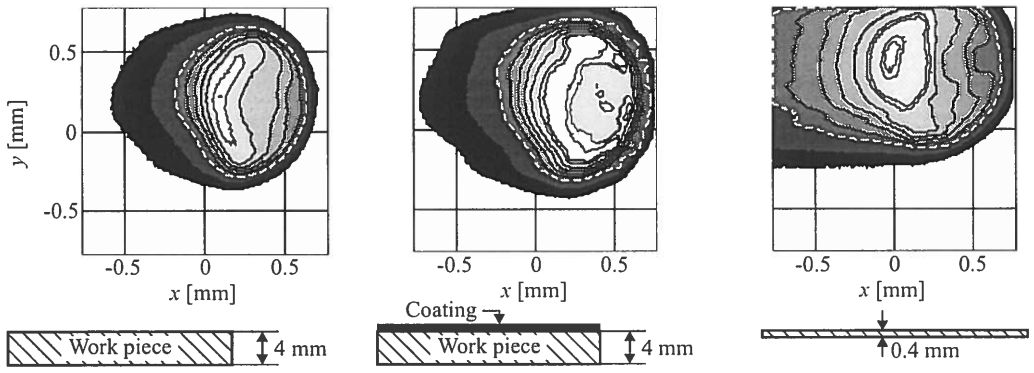

(a) Unperturbed. (b) High absorptivity. (c) Thin work piece.

Figure 3: Temperature contour plots (isotherms) of the laser material interaction zone and a schematic cross-sectionof the work piece (bottom). The dotted white line indicates the solid-liquid interface. Processing conditions: $P_L = 1000\,W$, $v = 50\,mm/s$.

of the temperature distribution is increased, and not its shape—i.e. the increase of the length and the width of the melt pool are of the same order. This conclusion was drawn already, based on equation

(1). Comparing to figure 3(a), the length of the melt pool in the thin work piece (fig. 3(c)) increases more than its width. This was also concluded based on figure 1.

Figure 4 shows the temperature in the center of the melt pool and the pool surface area S_m, when varying the laser power. The relative increase of the melt pool area is more significant than the

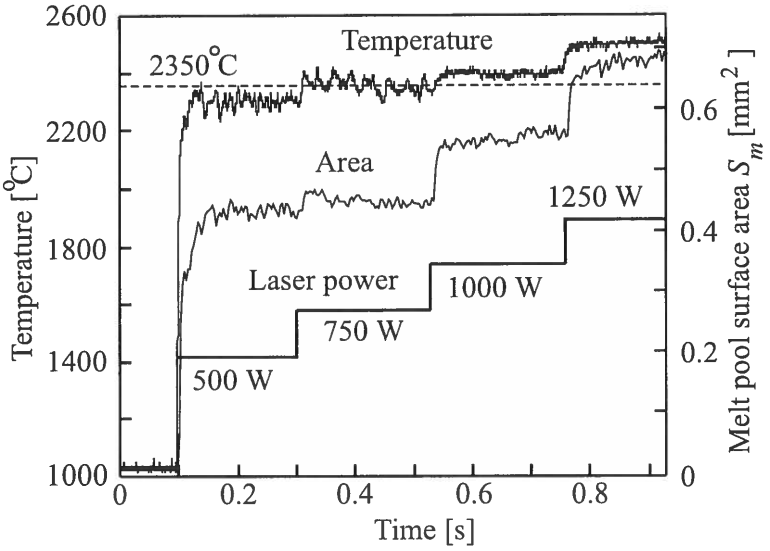

Figure 4: Melt pool temperature (as measured by the ratio pyrometer), the melt pool surface area (as measured by the thermographic camera) as functions of time, due to a step wise variation of the laser power, $v = 50\,mm/s$. The temporal response resembles the response of a first order process.

increase of its temperature. This means that the melt pool surface area has to be used for feedback control. But from experiments, in which the melt pool area S_m was controlled, it was found that the temperature of the melt pool can not be ignored entirely.[5] Therefore the spectral pyrometer was applied in a way such that is measures both pool area and temperature by overlapping the diameter of the melt pool by a factor 2. With this configuration, the signal variations of a spectral pyrometer, are caused mainly (65%) by a variations of the pool surface area, and (35%) by variations of its temperature.[5] The corresponding signal of the spectral pyrometer will be referred to as the melt pool "area" $S_{m,T}$ and is used for the control of laser alloying of Ti6Al4V (section 5).

It is possible to recognize geometrical and absorptivity disturbances. This is illustrated by figure 5, in which melt pool "area" $S_{m,T}$ and the temperature T_i directly behind the melt pool (measured by the ratio pyrometer) are shown. Because the measurement spot of the ratio pyrometer is aligned behind the melt pool it allows increase of the melt pool length to be detected. In the case of an absorptivity disturbance the relative increase of $S_{m,T}$ and T_i are approximately equal. Whereas, in the case of a geometrical disturbance, the relative increase of T_i is much larger than the relative increase of $S_{m,T}$. This is used for the design of a mode-switch controller (section 5). Due to the small dimensions of the thin region, the volume (including the surface area) of the melt pool increase and consequently the alloyed layer thickness.

Two transfer functions were determined by system identification: (*i*) a transfer function G_{P_L} relating the laser power to the melt pool "area", (*ii*) a transfer function relating the beam velocity to the temperature behind the melt pool. The system identification itself is nothing more than adjusting the parameters of the transfer function, such that the output of the model fits well with the measured series of inputs and outputs. MATLAB's system identification toolbox[10] was used for these calculations.

It is clear that the transfer function G_{P_L} (2) will not only include the process dynamics, but also

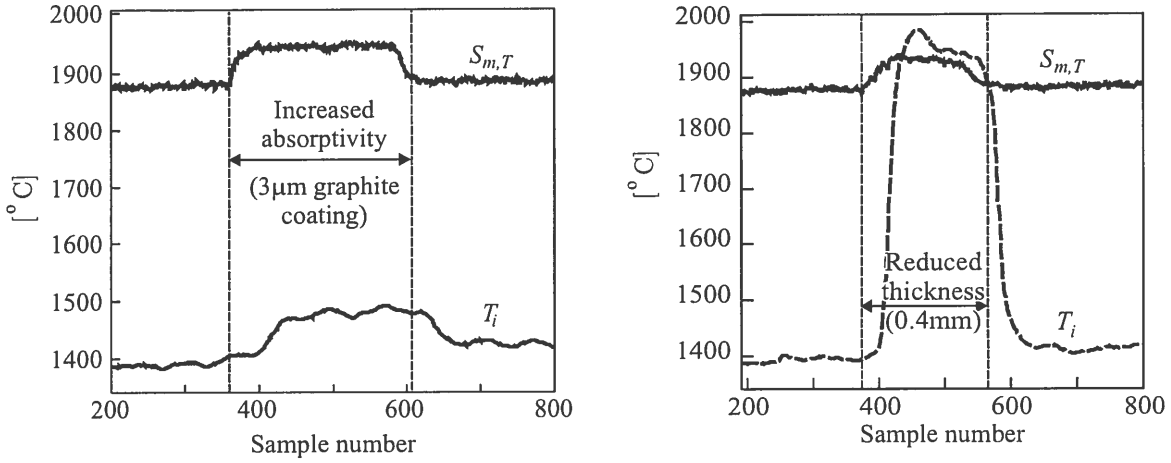

(a) Absorptivity disturbance.

(b) Geometrical disturbance.

Figure 5: Temporal response of the melt pool "area" $S_{m,T}$ and the temperature behind the melt pool T_i during process disturbances. Processing conditions: $P_L = 1250\,W$, $v = 40\,mm/s$.

the dynamics of the laser and the spectral pyrometer. The melt pool area depends non-linearly on laser power (fig. 4). Therefore, only small deviations (ΔP_L and $\Delta S_{m,T}$) of laser power and melt pool "area" around an operating point (P_{L0}, $S_{m,T0}$) are considered ($P_L = P_{L0} + \Delta P_L$ and $S_{m,T} = S_{m,T0} + \Delta S_{m,T}$). The model relating ΔP_L to $\Delta S_{m,T}$ is an *Auto Regressive eXogenous* (ARX) model, defined as[10]

$$G(q) = \frac{\Delta S_{m,T}}{\Delta P_L} = q^{-n_k}\frac{B(q)}{A(q)} + \frac{w}{A(q)}, \tag{4}$$

where $A(q) = 1 + a_1 q^{-1} + \cdots + a_{n_a} q^{-n_a}$ and $B(q) = b_0 + b_1 q^{-1} + \cdots + b_{n_b} q^{-n_b}$ are polynomials of orders n_a and n_b, in the backward shift (or delay) operator q^{-1}, while w represents white noise. The process delay n_k is expressed in number of sample periods ($1/f_s$). This delay is caused by communication delays, which were found to be constant and which could easily be eliminated from the measured signals and n_k was set to zero. As mentioned before the temporal response of the melt pool area resembles the response of a first order system ($n_a = 1$ and $n_b = 0$). However, it was found that the model parameters a_1 and b_0 depend on the operating point because of the non-linearity of the process.[5] A smooth and shiny titanium-nitride surface layer is obtained for beam velocities around 40mm/s and laser power around 1250W.[9] For this operating point, and a sample frequency of 550Hz the model parameters were found as $b_0 = 0.07034$ and $a_1 = -0.743$. With these parameters, the *Mean Square Fit* (MSF), which is a measure for the error between the model output and the measured data, is only 0.4% of $S_{m,T0}$.

For the design of a multivariable controller, the ARX model relating the beam velocity v to the temperature T_i behind the melt pool is required. System identification showed that this transfer function is best described by

$$G_v(q) = \frac{\Delta T_i}{\Delta v} = \frac{0.037184q^4 + 1.777q^3 + 1.473q^2 + 2.383q - 2.855}{q^4 - 1.611q^3 + 1.331q^2 + 0.6778q + 0.2089} \tag{5}$$
$$v_0 = 50.6\,\mathrm{mm{\cdot}s^{-1}},\ T_{i0} = 1644\,^\circ\mathrm{C},\ P_{L0} = 1250\,\mathrm{W},\ f_s = 157\,\mathrm{Hz},$$

where (v_0, T_{I0}) is the operating point. Because the bandwidth of the XY-table (50Hz) is small compared to the bandwidth of the thermal process, the third order dynamics of the XY-table are dominant

in (5). The sample frequency of (only) 157Hz was therefore chosen accordingly. Nevertheless, the model is sufficiently accurate as the MSF = 52.1 °C is only 3% of the operating point T_{i0}.

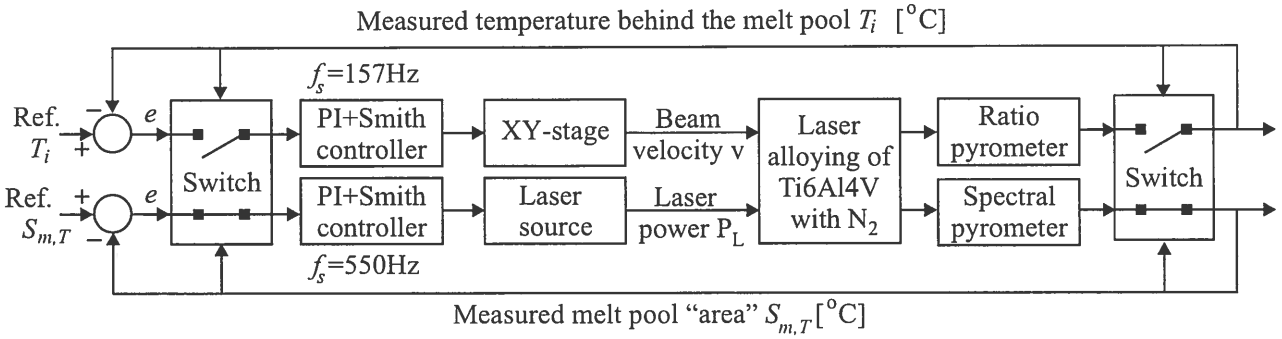

Figure 6: Block diagram of the laser alloying process controlled by the mode-switch controller. In the situation shown, the lower control loop is active.

5 Controller design & experimental results

Based on the results as described before, a multivariable mode-switch controller has been implemented.[11] The melt pool area was controlled by using the laser power as input command and the temperature T_i was controlled by using the beam velocity v. Figure 6 shows the corresponding block diagram. Depending on the state of the *switch* either the upper or lower control loop is active. The switch, determining which of the two control loops is active, was defined as

$$\text{Switch}: \begin{cases} \text{Control of } S_{m,T} & \text{by actuation of } P_L & \text{if } \Psi > 1 \\ \text{Control of } T_i & \text{by actuation of } v & \text{if } \Psi \leq 1 \end{cases}, \Psi = \frac{23\left|S_{m,T}/S^r_{m,T}\right|}{20\left|T_i/T^r_i\right|} \tag{6}$$

in which Ψ denotes the *mode-indicator* and where $S^r_{m,T}$ and T^r_i denote the reference values of the melt pool "area" and the temperature behind the melt pool, respectively. Each mode is controlled by its own controller. To guarantee a zero steady state error for step like disturbances (at the process input as well as output) a simple PI-controller,

$$C_{PI}(q) = K_P\left(1 + K_I(q-1)^{-1}\right) \tag{7}$$

suffices, where K_P denotes the proportional gain, $\tau_i = (K_I f_s)^{-1}$ the integration time of the integrator, f_s the sample rate, and K_I the integrator gain. Further, the PI-controller was augmented with a Smith-predictor[12] to allow high feedback gain despite communications delays. The controller parameters were tuned by a simulation of the controlled process using SIMULINK, which is toolbox of MATLAB for simulation of dynamical systems.

The controller parameters (K_P, K_I) corresponding to the lower loop in figure 6 were tuned such that a typical disturbance in absorptivity is eliminated in 35ms, with almost no overshoot. This was achieved with $K_P = 7.5$ and $K_I = 0.4$. The controller parameters corresponding to the upper loop were tuned such that a stepwise disturbance in work piece thickness (fig. 5(b)) is eliminated with reasonable speed, with no overshoot. This was achieved with $K_I = 0.35$ and $K_P = -0.03$. Both controllers were implemented in the CNC Work Station Controller (fig. 4).

When a mode-switch is detected, one of the controllers is activated and the other controller is de-activated. When the controller switches from laser power actuation to beam velocity actuation ($\Psi \leq 1$), a constant laser power level, equal to the level just before the switch, is applied to prevent an

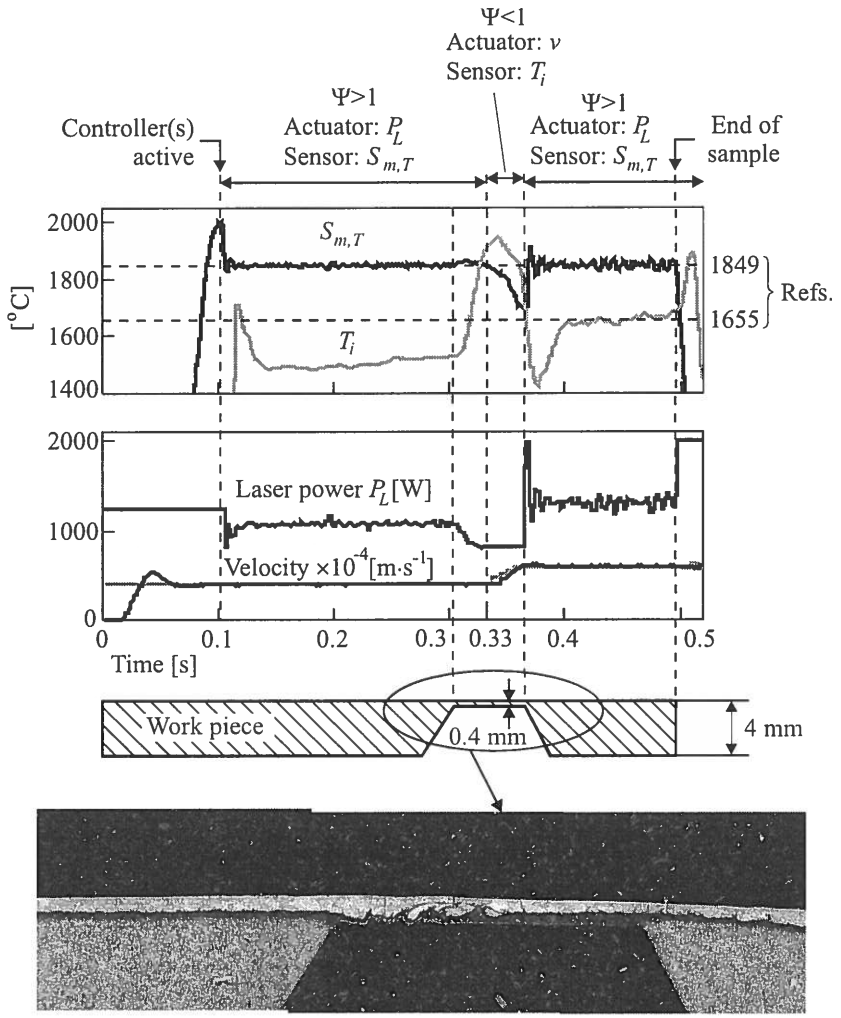

Figure 7: Performance of the mode-switch controller process during a geometrical disturbance. Measured input and output signals (top). Longitudinal-section of the work piece (bottom).

undesirable bump in the signal. In addition, the error signal corresponding to the melt pool "area" is set to zero: $e(k) = S^r_{m,T} - S_{m,T} = 0$. However, this does not guarantee a bumpless transfer from laser power actuation to beam velocity actuation. Figure 7 shows the performance of the mode-switch controller during treatment of a work piece with a stepwise variation in thickness. First, the process is controlled by actuation of the laser power. At $t = 0.3$ s a disturbance was detected, but not yet identified as the geometrical disturbance, so first the laser power was reduced. From $t = 0.33$ s, the geometrical disturbance is detected and the process is controlled by steering the velocity. At $t \approx 0.36$ s the geometrical disturbance ends, and the controller switches back to control of the "area" by steering the laser power. As can be observed from longitudinal-section of the work piece, the alloyed layer thickness increases first, but it then reduces to the desired thickness. This test demonstrates the capabilities of the multivariable mode-switch controller. Even under these extreme conditions the controlled process is stable, while in all other cases a melt through of the thin bridge was observed.

References

[1] W. Bloehs, D. Grünenwald, F. Dausinger, and H. Hügel. Recent progress in laser surface treatment: I. Implications of laser wavelength. *Journal of laser applications*, 8:15–23, 1996.

[2] W. Kurz and R. Trivedi. Microstructure selection in laser treatment of materials. In *Proceedings of the ECLAT'88*, pages 92–94, 1988.

[3] A. Zambon, E. Ramous, M. Magrini, M Bianco, and C. Rivela. Gas surface alloying of Ti6Al4V alloy by laser. In *Proceedings of the NATO advanced study institute on laser processing, Sesimbra, Portugal, july 3-16*, pages 327–335, 1994.

[4] C. Lampa. An analytical thermodynamic model of laser welding. *Journal of physics, Section D, Applied physics*, 30:1293–1299, 1997.

[5] G.R.B.E. Römer. *Modelling and control of laser surface treatment.* PhD thesis, University of Twente, Enschede, the Netherlands, 1998.

[6] E. Zauderer. *Partial differential equations of applied mathematics.* Wiley, Chichester, U.K., 1989.

[7] G.R.B.E. Römer, R.G.K.M. Aarts, and J. Meijer. Dynamic models of laser surface alloying. *Lasers in engineering*, 8(4):251–266, 1999.

[8] G.R.B.E. Römer, M. Hoeksma, and J. Meijer. Industrial imaging controls laser surface treatment. *Photonics Spectra*, 11:104–109, 1997.

[9] G.R.B.E. Römer and J. Meijer. Analytical model describing the relationship between laser power, beam velocity and melt pool depth in the case of laser (re)melting, -alloying and -dispersing. In *Proceedings of the conference on lasers in material processing EUROPTO/SPIE, vol. 3097*, pages 507–515, 1997.

[10] L. Ljung. *User's guide system identification toolbox for use with* MATLAB. The Mathworks Inc., Natick, U.S.A., 1995.

[11] R.A. Hilhorst. *Supervisory control of mode-switch processes.* PhD thesis, University of Twente, Enschede, the Netherlands, 1992.

[12] O.J.M. Smith. A controller to overcome dead time. *ISA journal*, 6:28–33, 1959.